Fermi National Accelerator Laboratory

FERMILAB-Conf-88/69

Coherent Betatron Instability in the TEVATRON*

S. A. Bogacz, M. Harrison, and K.-Y. Ng
Accelerator Theory Department
Fermi National Accelerator Laboratory
P.O. Box 500, Batavia, Illinois 60510

June 9, 1988

*To be presented at the European Particle Accelerator Conference, Rome, Italy, June 7-11, 1988

COHERENT BETATRON INSTABILITY IN THE TEVATRON

S.A. Bogacz, M.Harrison and K.Y. Ng
Accelerator Theory Department, Fermi National Accelerator Laboratory, P.O. Box 500, Batavia, IL 60510, USA

Beam Instability - Observations

The instability was first observed during the recent 1987–88 Tevatron fixed target run. In this operating mode 1000 consecutive bunches are loaded into the machine at 150 GeV with a bunch spacing of 18.8 $\times 10^{-9}$ sec (53 MHz). The normalized transverse emittance is typically 15 $\pi \times 10^{-6}$ m rad in each plane with a longitudinal emittance of about 1.5 eV-sec. The beam is accelerated to 800 GeV in 13 sec. and then it is resonantly extracted during a 23 sec flat top. As the run progressed the bunch intensities were increased until at about 1.4 $\times 10^{10}$ ppb (protons per bunch) we experienced the onset of a coherent horizontal oscillation taking place in the later stages of the acceleration cycle (> 600 GeV). This rapidly developing coherent instability results in a significant emittance growth, which limits machine performance and in a catastrophic scenario it even prevents extraction of the beam.

The characteristics of the instability are as follows: It was only observed in the horizontal plane and at the higher energies, we were unable to detect any obvious longitudinal modes. There was a relatively strong intensity threshold; 10% changes in bunch intensity would completely eliminate the effect. The oscillation was self-stabilizing at the 2–3 mm betatron amplitude level. The effect was non-resonant with no strong dependance on the tune. The intensity threshold could be increased by reducing the chromaticity to be positive but close to zero (1–2 units) but there was no dramatic sensitivity to chromaticity.

The most successful method of raising the intensity threshold was achieved by increasing the longitudinal emittance by applying white noise to the rf drive, an emittance of 5 eV-sec. would permit a bunch intensity of about 1.8 $\times 10^{10}$ ppb. The growth time was fast; less than 30 $\times 10^{-3}$ sec. Typically, the full ring would go unstable, but we have observed unstable behavior in a partial azimuth of the ring when bunches of significantly higher intensity were present. Attempts at Landau damping with octupole circuits had no great effect but our ability to do this was hampered by the fact that the value of the octupoles at flattop was constrained by the resonant extraction process.

The instability was characterized by a strong low frequency signal at the first betatron sideband of the revolution frequency (~ 25 kHz). This is shown in Fig.1, which is the output from a beam position monitor showing the beam position over 10 turns. The tick marks represent the gap in the circulating beam, which is coming once per revolution. Using a wide band pickup (2 GHz) we attempted to identify any higher frequency components such as those expected from intrabeam oscillations. While these measurements are difficult to make, we were unable to see any strong evidence for higher order modes within the bunches, which we would have expected in the 500 – 900 MHz region.

In the next few sections, we will present a simple analytic description of the observed instability. We will show that a combination of a resistive wall coupled bunch effect and a single bunch slow head-tail instability is consistent with the above observations. Finally, a systematic numerical analysis of our model (growth-time vs chromaticity plots) points to the existence of the $\ell \geq 1$ slow head-tail modes as a plausible mechanism for the observed coherent instability. This last claim, as mentioned before, does not have conclusive experimental evidence, although it is based on a very good agreement between the measured values of the instability growth-time and the ones calculated on the basis of our model.

Single Particle Equation of Motion - Growth Time

Following Sacherer's argument[1] one can generalize a simple equation of motion describing a wake field driven coherent betatron motion of a coasting beam to model the head-tail instability of the bunched beam. A simple dipole oscillation of the coasting beam as a whole is governed by the following equation

$$\ddot{x} + (\nu\omega_o)^2 x = i\frac{e\beta}{\gamma m_o}\ \frac{Z_\perp I}{2\pi R}\ x\ . \tag{1}$$

Here x is the transverse displacement, $Z_\perp$ denotes the transverse coupling impedance, I is the total beam current and R is the machine radius. The following approach assumes ad hoc existence of a given head-tail mode, ℓ, by imposing specific periodic dependence of the betatron motion with respect to the longitudinal

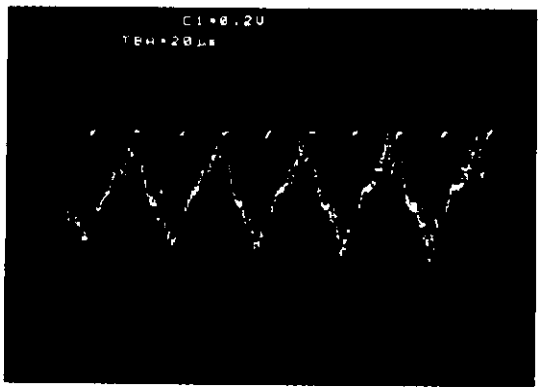

Fig.1 Output from a beam position monitor showing the transverse beam position over 10 turns

position, τ.

In a case of a bunched beam the wake field experienced by a test particle at the position τ is now given by the following convolution of the transverse impedance and the normalized beam spectrum, ρ

$$V^\ell(\tau) = \omega_o \sum_{p=-\infty}^{\infty} Z_\perp(\omega_p)\ \rho^\ell(\omega_p - \omega_\xi)\ e^{\,i\omega_o\tau p}\ , \tag{2}$$

where the beam spectrum for a given mode is defined as follows

$$\rho^\ell(\omega) = \frac{h^\ell(\omega)}{\sum_{p=-\infty}^{\infty} h^\ell(\omega_p)}\ . \tag{3}$$

The explicit form of the power spectrum is given by the following expression

$$h_\ell(\omega) = \frac{4}{\pi^2}\ (\ell+1)\ \frac{1 + (-1)^\ell \cos(2\omega\hat{\tau})}{[(2\omega\hat{\tau}/\pi)^2 - (\ell+1)^2]^2}\ . \tag{4}$$

The deflecting transverse wake force acting on the particle is a sum of the wakes generated by all the particles in the bunch, which are ahead of the test particle (causality); it also includes long range wakes left from all the preceding turns. The last feature is explicitly built into the definition of $V^\ell(\tau)$, given by Eq.(2). Resulting transverse wake force is conveniently expressed by the following integral

$$F^\ell(\tau) = i\frac{e\beta}{\gamma m_o}\ \frac{I_o}{2\hat{\tau}c}\ \int_{\tau}^{\hat{\tau}} d\tau'\ V^\ell(\tau')\ h^\ell(\tau')\ . \tag{5}$$

Substituting the above expression in the RHS of Eq.(1)one obtains after a little algebra a complete equation of motion for the ℓ-th head-tail mode, defining. The imaginary part of the coherent frequency of the ℓ-th mode(with the negative sign) represents the inverse growth-time and is expressed by the following formula

$$\frac{1}{\tau^\ell} = -\frac{ce\beta I_o}{4\pi E\nu}\ \mathrm{Re}\ Z_{\mathrm{eff}}^\ell\ , \tag{6}$$

where $E = \gamma m_o c^2$ is the total energy and Z_{eff}^ℓ is the effective impedance defined as follows

$$Z^{\ell}_{eff} = \frac{2\pi}{\ell+1}\,\frac{1}{2\omega_o\hat{\tau}}\sum_{p'=-\infty}^{\infty} Z_\perp(\omega_{p'})\,\rho^{\ell}(\omega_{p'}-\omega_\xi) \qquad (7)$$

The above result can be compared with the growth-time obtained in the framework of the Vlasov equation-based description of the slow head-tail instability. The so-called "air bag" model[2] assumes δ-like shell structure of the longitudinal phase-space, which serves as the equilibrium density distribution function (on top of which various head-tail modes are constructed as small fluctuations of the particle density). The resulting formula has exactly the same generic form as given by Eq.(6) with the effective impedance introduced as an average over different set of spectral density functions; namely the Bessel functions of the first kind. This average is given explicitly as follows

$$Z^{\ell}_{eff} = \sum_{p'=-\infty}^{\infty} Z_\perp(\omega_{p'})\,J^2_\ell((\omega_{p'}-\omega_\xi)\hat{\tau}). \qquad (8)$$

To remove model dependence from our study both results will be applied to carry out model calculation of the specific head-tail instability in the Tevatron. The results of the next sections show clearly that there is very little difference between both models.

Transverse Coupling Impedance

Our consideration will be confined to the real part of the impedance only, since the imaginary part does not enter explicitly into the growth-time formulae given by Eqs.(6) and (7). We tentatively identified four dominant sources of the transverse impedance. These potentially offending vacuum structures can be listed as follows

(a) bellows
(b) kicker magnets
(c) beam position monitors
(d) resistive wall and magnet laminations.

(a) The first contribution was estimated numerically using the TBCI code (real time solution of the Maxwell equations for a given geometry excited by a Gaussian test bunch). Calculated Fourier transform of the transverse wake field is translated into the transverse impedance in Ohm/m. The solution can be fitted into a broad-band resonance parametrized by the shunt impedance R_{sh}, the quality factor Q and the resonant frequency ω_c. The resulting fit is summarized by

$$Z_\perp(\omega) = \frac{R_{sh}\;\omega/\omega_c}{1 + iQ(\omega/\omega_c - \omega_c/\omega)}\ , \qquad (9)$$

where

$R_{sh} = 1.2 \times 10^6$ Ohm/m
$Q = 3.3$
$\omega_c = 2\pi \times 9.1$ GHz.

(b) There are eleven kicker magnets; both injection and abort kickers located around the ring. According to Ref.3 the real part of the transverse coupling impedance of a c-magnet of half-width a, half-height b and length L is given by the following analytic expression

$$\mathrm{Re}\,Z_\perp(\omega) = \frac{Z_o L}{4ab}\,\frac{1}{\omega}\,\left(1-\cos\frac{\omega L}{c}\right)\ , \qquad (10)$$

where

$Z_o = 377$ Ohm
$L = 1$ m
$a = 3.7$ cm
$b = 1.9$ cm.

(c) Similar contribution comes from 108 beam position monitors. Each unit consists of a pair of cylindrical strips of length ℓ and width $b\phi_o$ forming a simple transmission line of the characteristic impedance Z_s. The real part of the transverse impedance is expressed as follows[3]

$$\mathrm{Re}\,Z_\perp(\omega) = \frac{8Z_s}{\pi^2 b^2}\,\frac{c}{\omega}\,\sin^2\frac{\phi_o}{2}\,\sin^2\frac{\omega\ell}{c}\ , \qquad (11)$$

where

$\ell = 18$ cm
$Z_s = 50$ Ohm
$b = 3.5$ cm
$\phi_o = 1.92$ rad.

(d) Finally, the low frequency contribution to the transverse impedance due to the resistive wall and Lambertson magnet laminations is given by the following standard expression[4]

$$Z_\perp(\omega) = (1+i)\frac{W}{\omega/\omega_o}\ , \qquad (12)$$

where

$W = 2.3 \times 10^6$ Ohm/m.

All four contributions will serve as a starting point for calculation of the effective impedance which will be carried out in the next section.

Effective Impedance

In order to evaluate the effective impedance one has to convolute the above four contributions to the transverse impedance with the beam spectrum according to Eqs.(7) and (8).The result of the above summation obviously depends on chromaticity. The resistive wall contributes only one term; either evaluated at $\nu\omega_o$ or at $(1-\nu)\omega_o$ This is a consequence of the fact that for any neighboring sampling frequency the transverse impedance is negligibly small (hyperbolic tail). Therefore, only one spectral line at very low frequency (~ 25 kHz) couples to the resistive wall impedance causing existence of the stationary long range pattern depicted in Fig.2. Coherent motion of individual bunches is coupled due to the presence of long range wake field which leads to this low frequency correlation of the betatron amplitudes defining transverse motion of the bunch centroids[4].

One can notice that for both contributions (b) and (c) their transverse impedances $Z_\perp(\omega)$, given by Eqs.(10) and (11), have a diffraction-like character; a principle maximum of width $\lambda = \pi c/L$ at the origin and a series of equally spaced secondary maxima governed by the same width. Similarly, the harmonics of the beam spectrum, $\rho^{\ell}(\omega-\omega_\xi)$, have one ($\ell = 0$) or a pair ($\ell \geq 1$) of principle maxima of width $\varepsilon = \pi/2\hat{\tau}$ followed by a sequence of secondary maxima Both spectra are sampled by a discrete set of frequencies, $\omega_p = (p+\nu)\omega_o$. In case of relatively long proton bunches in the Tevatron at 800 GeV ($2\hat{\tau} = 2 - 3 \times 10^{-9}$ sec) both widths λ and ε

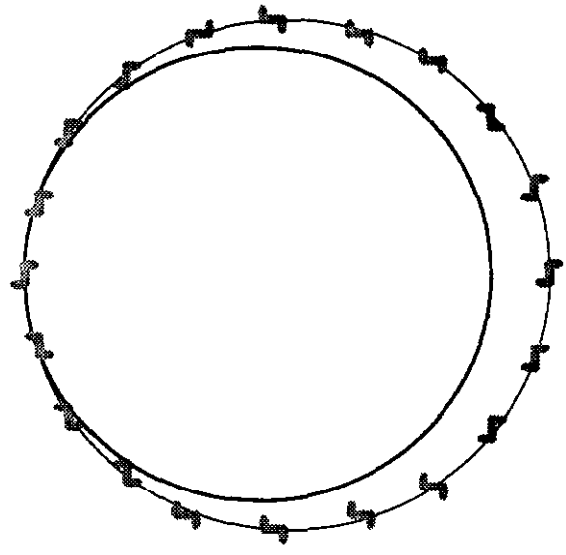

Fig.2 Schematic diagram of the resistive wall coupled bunch instability combined with the slow head-tail $\ell = 1$ mode - suggested picture of the observed coherent betatron instability

are comparable and they are of the order of the chromatic frequency, ω_ξ, evaluated at about 10 units of chromaticity. These features combined with the convolution formula for the effective impedance, Eqs.(7) and (8), result in substantial 'overlap' of the transverse impedance and the beam spectrum, which in turn leads to large values of effective impedance for relatively small chromaticities ($\xi \sim 10$).

In contrast, the effective impedance evaluated with the broad-band part (a) of the transverse impedance is much smaller than the previously discussed one. The last statement can be explained as follows; the width of the broad-band impedance peak, $\delta = \omega_c/Q$, is much larger than ε and in order to overlap this broad peak with the principal maximum of the power spectrum harmonics (to get a nonzero effective impedance) one would have to shift both spectra by ω_ξ of the order of δ. This, in turn, would require enormous values of the chromaticity ($\xi \sim 10^4$).

Summarizing, only two out of four contributions to the transverse impedance are relevant to the discussed coherent betatron instability. First, the resistive wall part, which couples to the low frequency (~ 25 kHz) single spectral line is responsible for the observed coupled bunch pattern. Second, the kicker magnet contribution driving high frequency band of several lines centered around 500 MHz is in turn responsible for single bunch slow head-tail modes. The similar coupling due to the beam position monitors is much weaker, because of the small absolute value of the transverse impedance and therefore is neglected in further consideration.

Conclusions

At this point some the comparison of numerically evaluated results of the presented model with the observed coherent instability is in order. Assuming only two dominant contributions to the transverse coupling impedance; resistive wall given by Eq.(10) and kicker magnets expressed by Eq.(12), the inverse growth-time was calculated numerically according to Eqs.(6)–(8). The resulting growth-rate as a function of chromaticity evaluated for different slow head-tail modes ($\ell = 0, 1, 2, 3$) are illustrated in Fig.3. One can immediately see a qualitative difference between the $\ell = 0$ and $\ell > 1$ modes; the resistive wall effect is much more dramatic for $\ell = 0$ mode and leads to strong instability even at zero chromaticity. Higher order modes, on the other hand, are only slightly effected by the resistive wall coupling.

The experimentally observed situation corresponds to chromaticity of about 15 units. Fig.3 shows that $\ell = 1$ mode is strongly unstable with the growth-time of about 40×10^{-3}sec, which would suggest that this mode is responsible for the observed betatron instability. One way of suppressing the $\ell = 1$ mode would be by decreasing chromaticity. This scheme has been successfully tried during the last fixed target run. However, as one can see from Fig.3, the $\ell = 0$ mode appears to be unstable for small positive chromaticities and might lead to significant enhancement of coherent betatron motion due to previously discussed resistive wall coupling. Fortunately, this potentially offending mode can be effectively suppressed by the active damper system also employed during the last fixed target run. This efficient cure for the $\ell = 0$ mode obviously does not work in case of the higher modes, since its feedback system picks up only the transverse position of a bunch centroid, which remains zero due to the symmetry of the higher modes. Another possible cure (also effective for the $\ell \geq 1$ modes) would involve the Landau damping through the octupole-induced betatron tune spread. Increasing betatron amplitude of initially unstable mode causes increase of the tune spread, which will eventually self-stabilize development of this mode. The efficacy of this last scheme will be examined in the next fixed target run.

In conclusion, we identified observed coherent instability as a combination of the single bunch slow head-tail modes driven by the kicker magnets and the coupled bunch resistive wall instability. Good agreement between the measurements and the growth-times

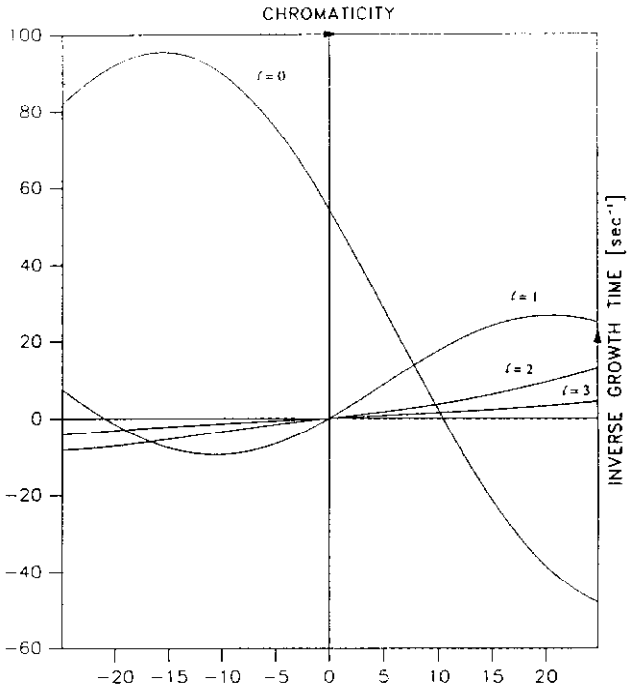

Fig.3 A family of inverse growth-time vs chromaticity curves evaluated numerically for various head-tail mode indices ℓ

calculated within the framework of the presented model points strongly at the $\ell = 1$ mode as the offending single bunch component of the observed instability. Whether this picture is really true, or perhaps the $\ell = 0$ mode is present instead; this question should be addressed through a detailed high resolution real time observation carried out in the next run.

References

[1] F. Sacherer, Proc. 9-th Int. Conf. on High Energy Accelerators, Stanford 1974, p. 347

[2] F. Sacherer, CERN/SI-BR/72-5 (1972), unpublished

[3] K.Y. Ng, Principles of the High Energy Hadron Colliders, Part I, edited by A.W. Chao and M. Month (1987)

[4] L.J. Laslett, V.K. Neil, A.M. Sessler, Rev. Sci. Instr., **36**, (1965), p. 436